A Triboscopic Investigation of the Wear and Friction of MoS_2 in a Reciprocating Sliding Contact

K.J. Wahl[a], M. Belin[b], and I.L. Singer[a]

[a]*Code 6176, Naval Research Laboratory, Washington DC 20375-5342*
[b]*Laboratoire de Tribologie et Dynamique des Systèmes, Ecole Centrale, BP 163, F-69131 Ecully, Cedex, France*

Abstract

Reciprocating sliding tests with ball-on-flat geometry were performed on a duplex coating at low speeds in moist air (RH=60%). The coating, 55 nm MoS_2 on 35 nm of TiN, was deposited by ion-beam assisted deposition onto a steel substrate. Friction coefficient (μ) and electrical contact resistance (R_c) measurements were recorded at ~2μm intervals along the track; these spatially resolved measurements were compared to the more commonly presented cycle-averaged values. The last-cycle tracks of several runs were also analyzed by a variety of microscopies and spectroscopies to identify compositions and determine thicknesses of films on the tracks and balls. R_c measurements, both averaged and spatially resolved, were more sensitive to coating damage and loss than μ measurements. In the averaged data, fluctuations in R_c were observed before fluctuations in μ. Spatially resolved data showed that local drops in R_c could be detected as early as 20% of life. Additionally, recovery of both high μ and low R_c regions, interpreted as healing of damage in the contact, occurs. Friction coefficient data were insensitive to changes in MoS_2 coating thickness; conversely, R_c followed wear track thickness and consequently may provide an *in situ* method of monitoring coating wear.

Submitted to Wear: 21 July 1997; Accepted: 8 October 1997

Report Documentation Page

Form Approved
OMB No. 0704-0188

1. REPORT DATE	2. REPORT TYPE	3. DATES COVERED
1997		**00-00-1997 to 00-00-1997**

4. TITLE AND SUBTITLE	5a. CONTRACT NUMBER
A Triboscopic Investigation of the Wear and Friction of MoS2 in a Reciprocating Sliding Contact	5b. GRANT NUMBER
	5c. PROGRAM ELEMENT NUMBER
6. AUTHOR(S)	5d. PROJECT NUMBER
	5e. TASK NUMBER
	5f. WORK UNIT NUMBER
7. PERFORMING ORGANIZATION NAME(S) AND ADDRESS(ES) **Naval Research Laboratory,Code 6176,4555 Overlook Avenue, SW,Washington,DC,20375**	8. PERFORMING ORGANIZATION REPORT NUMBER
9. SPONSORING/MONITORING AGENCY NAME(S) AND ADDRESS(ES)	10. SPONSOR/MONITOR'S ACRONYM(S)
	11. SPONSOR/MONITOR'S REPORT NUMBER(S)

12. DISTRIBUTION/AVAILABILITY STATEMENT
Approved for public release; distribution unlimited

13. SUPPLEMENTARY NOTES
The original document contains color images.

14. ABSTRACT

15. SUBJECT TERMS

16. SECURITY CLASSIFICATION OF:			17. LIMITATION OF ABSTRACT	18. NUMBER OF PAGES	19a. NAME OF RESPONSIBLE PERSON
a. REPORT **unclassified**	b. ABSTRACT **unclassified**	c. THIS PAGE **unclassified**		**25**	

1. Introduction

Understanding the conditions within a sliding contact (including changes in thickness of the film separating the interfaces, composition of films, loss of material as debris, etc.) is a complicated task due to the "buried" nature of the interface. Often, friction coefficient is the only method to monitor the condition of a sliding contact during an experiment. For thin solid lubricant films such as MoS_2, the friction coefficient can be remarkably stable, despite the fact that much of the MoS_2 coating is worn early in the life of the contact [1-6]; this stability makes it difficult to sense coating loss using friction or torque signals [7,8]. The friction stability has been attributed to replenishment of the contact by transfer of worn MoS_2 [3,4,9] from lubricant reservoirs [6,10] and to the need for only a few layers of MoS_2 to sustain low μ [11].

An additional means of monitoring the condition of a sliding contact is through measuring the electrical contact resistance (R_c) of the sliding interface. R_c measurements previously have been used to investigate area of contact, stick/slip events and breakdown of hydrodynamic lubrication [e.g. 12-14]. Contact resistance of solid lubricants in metallic composites [15] as well as burnished films of MoS_2 [16] have also been studied. Belin and Martin [17] recently demonstrated that complementary pictures of the condition of the contact can be obtained by simultaneous recording of spatially resolved electrical contact resistance and friction measurements. The technique, called "triboscopy," monitors the evolution of time dependent local phenomena (e.g. breakthrough of a non-conductive coating), with a spatial resolution limited by contact size.

The purpose of this study is to investigate the ability of triboscopy to monitor the sliding wear behavior of MoS_2 coatings. Triboscopic data were acquired from a MoS_2 coating that was very thin in order to allow accelerated wear testing; sliding tests ranged from 512 to 2048 cycles. After testing at steady state as well as to failure, selected worn ball and track surfaces were characterized with *ex situ* surface analyses. The surface analytical results, combined with the triboscopic data, allowed interpretation of the last cycle μ and R_c data in terms of wear, material transfer, and chemistry of the sliding interface. General observations from the triboscopy experiments will be presented. Additionally, we will use what we learned from this combination of

techniques to make inferences about the history of the wear process, as well as the potential of R_c measurements for prediction of wear and lubricant failure.

2. Experimental procedure

2.1. Coating Deposition

A duplex MoS_2 coating was deposited by ion-beam assisted deposition (IBAD) to a thickness of 55 nm on a TiN-coated 440C steel substrate [18]. MoS_2 deposition conditions (200°C, ion-to-atom ratio 0.4) were chosen to obtain a preferred basal orientation (the (001) planes parallel to the substrate), as determined by X-ray diffraction [19]. The thin (35 nm) layer of TiN was deposited on the steel to act as a diffusion barrier [20].

2.2. Tribological Characterization

Reciprocating ball-on-flat sliding experiments were performed in ambient air (60% RH) using 6.35 mm diameter 52100 steel balls. The sliding speed was 0.66 mm/s over a stroke (track) length of 1 mm. Loads of 4.0 and 10.0 N were used. Under these conditions, the maximum Hertzian pressures were 1.0 and 1.4 GPa and Hertzian contact diameters 88 and 120 μm, respectively. The very thin MoS_2 coating and high relative humidity environment were chosen to allow accelerated testing, as both high humidity [21] and reduced lubricant thickness [4,22] are known to decrease the endurance of MoS_2 coatings. Eleven sliding experiments were run, to a maximum of 2048 cycles; two of these will be presented in detail here.

The reciprocating sliding test apparatus used for these experiments monitors both tangential force and electrical contact resistance and has been described previously [17]. Briefly, friction and resistance signals are acquired with a computer programmed to sample and store data at equal time intervals during the forward sliding cycle. The time intervals are then converted to displacement intervals to establish the relative position along the track; however, this leads to slight misrepresentation of position because the finite stiffness of the measurement arm delays onset of sliding.

In this paper, the data are presented in two ways. First, data for each sliding cycle are averaged then presented in the traditional format of μ^{av} vs. cycle and log R_c^{av} vs. cycle. Secondly, μ and log R_c values are presented using a greyscale map format, called “triboscopic” images: data

as a function of wear track position are shown on the horizontal axis and as a function of sliding cycle on the vertical axis. The contrast in the images makes it easy to recognize changes along the track in a given cycle and at a given location on the track as sliding progresses. Contrast variations will be described in the text as either *local* (within a specific region of a track) or *global* (along the entire track).

The spatial resolution of the image is related to both the total number of data points acquired along the track length and the Hertzian contact zone. In these experiments, 512 data points were acquired along the track; therefore each pixel in the image corresponds to a ~2 μm increment along the track. However, the actual spatial resolution is a convolution of the corresponding pixel size and the contact area (in this case, the Hertzian diameter).

2.3. Surface Analyses

After the reciprocating sliding tests, wear tracks on the coated flat and ball wear scars were examined optically and with several surface analytical techniques. Micro-Raman spectroscopy was performed using a Renishaw imaging microscope equipped with a low-power Ar^+ laser (514 nm) operated at less than 25 mW to avoid oxidation of the material analyzed; spectrometer resolution was 1 cm^{-1} and the diameter of the spot analyzed was 2 μm. Compositions were inferred from spectra acquired with standard reference materials. Worn coating and ball transfer films were also examined using both a thin window Tracor Northern energy dispersive x-ray spectrometer (EDS) and a Physical Electronics PHI 660 scanning Auger microprobe (SAM); both instruments were housed in the same UHV chamber. EDS spectra were obtained at a beam energy of 10 keV, beam current 2.0 nA and detector take-off angle of 25°. Auger spectra were acquired using primary electron beam energies between 3 and 10 keV, and sputter depth profiling was performed with a 3 keV Ar^+ ion beam. Sensitivity factors supplied with the microprobe were used to obtain normalized Auger intensities. Integrated intensity of the overlapping Mo and S peaks from the EDS spectra were used to estimate the thickness of MoS_2 remaining in the wear tracks and transferred to the ball surfaces [23, 24].

3. Results and Discussion

3.1. Triboscopy of MoS_2

3.1.1. Evolution of averaged data

Figure 1a shows average friction coefficient (μ^{av}) vs. cycle for two sliding tests at 4.0 N load, stopped at 512 and 2048 sliding cycles. The friction coefficient rose during the first several hundred cycles, remained smooth and nearly constant (0.15) up to ~1000 cycles, dropped slightly then fluctuated somewhat up to ~1500 cycles. Finally, after ~1500 cycles, friction increased sharply and became erratic; but recovering several times to near 0.15.

Figure 1b shows average electrical contact resistance, R_c^{av}, vs. cycle recorded simultaneously with the friction measurements. After a rapid rise of as much as one order of magnitude during the first 100 cycles, R_c^{av} remained between 100 and 1000Ω, but fluctuated more than μ^{av}. At around 1000 cycles (where the friction dropped and began to fluctuate), R_c^{av} showed a larger drop and greater fluctuations than μ^{av}. At ~1300 cycles, R_c^{av} increased sharply and fluctuated over several orders of magnitude; these erratic fluctuations began several hundred cycles before similar fluctuations in μ^{av}.

3.1.2. Triboscopic images of m*and R_c*

Triboscopic images of the data presented in Fig. 1 are shown in Figs. 2 and 3. In the images, darker regions indicate lower values and lighter regions higher values of both μ and R_c (see calibration bars beneath images). Note that due to artifacts in the data acquisition, data at the edges of the images, acquired during the turn-around portions of sliding, are somewhat ragged and will be ignored.

Triboscopic friction images displayed very little contrast in the early stages of sliding. By 200 to 300 cycles, the left side of the images showed higher friction than the right for both the 512 (Fig. 2) and 2048 (Fig. 3) cycle tests, with friction on the left increasing as sliding continued. This is consistent with the observations of the μ^{av} data (Fig. 1a) early in sliding, where μ increased smoothly. Between ~1000 and 1500 cycles (Fig. 3), friction decreased slightly along the left side of the wear track periodically and at times the entire length of the track had low friction; this behavior corresponds to the region in the μ^{av} data when the friction suddenly dropped and became noisier. Finally, friction images occasionally displayed sharp increases in friction, either along all

or parts of the track length (see Fig. 3 at ~1530 cycles and beyond). Recovery of low friction in sections along the track (e.g. from ~200 to 800 μm between ~1650 and 1750 cycles, and ~1850 to the end of the test) correlates to drops in the μ^{av} data seen in Fig 1a.

The contact resistance images showed even more contrast variations than the friction images. Moreover, the variations began before changes in μ were observed. Early in sliding, the variations in R_c were sometimes quite large (over several orders of magnitude) along the length of the wear tracks (see Fig. 2, region A and Fig. 3, first 500 cycles); the increase, then decrease of R_c accounts for the early variation seen in the R_c^{av} data (Fig. 1b). Between ~1000 and 1300 cycles (Fig. 3), R_c was low on the right side of the image and periodically high in localized regions on the left side of the track; these localized increases result in increased noise in the corresponding R_c^{av} data. As sliding continued, sudden large increases in R_c across the entire image were observed (Fig. 3, ~1300 cycles); ~300 cycles later, R_c fell several orders of magnitude. This behavior was repeated and corresponds to the large (2-3 orders of magnitude) fluctuations in the R_c^{av} data.

An additional feature was observed in a number of the R_c triboscopy images (but not in the friction images): discrete, low R_c regions (generally < 10Ω) were seen as early as 300 cycles (see e.g. Fig. 2, region B, marked by small squares). Examples of the low R_c regions can be more clearly seen in another test run at a higher load (10 N), shown in Fig. 4. The first low R_c region can be found from ~350 and 380 cycles, on the right side of the track between ~750 and 800 μm. Between ~400 and 450 cycles, this low R_c region disappeared, but then reappeared at ~460 and ~500 cycles in essentially the same location along the track; by 700 cycles, low R_c regions covering even larger portions of the track were observed. These localized regions along the track exhibited recovery phenomena analogous to that observed in the friction data, returning to values consistent with other nearby (unaffected) regions. No changes in friction were associated with the discrete variations in R_c.

The triboscopic images resolved fluctuations in μ and R_c and pinpointed locations of these regions along the wear track; however, they do not reveal what physical processes caused these variations. Triboscopic results raised but did not answer several questions:

- What are the low resistance regions: are they different composition, or holes in the coating?

- How much coating wear has occurred, and can the coating thickness be inferred from either the μ or R_c data?

To answer the above questions, *ex situ* optical and chemical analyses of the worn surfaces were performed.

3.2. Characterization of worn surfaces

3.2.1. Analysis and interpretation of 512 cycle track

Figure 5 shows the last cycle μ and R_c data from the 512 cycle test shown in Fig. 2. Both μ and R_c varied across the track: μ was highest on the left side of the track, but had a minimum where R_c had a maximum on the right third of the track.

Optical micrographs of the worn ball and track surfaces are shown in Fig. 6. On the flat, the wear track was about 90 μm wide, consistent with the Hertzian calculation of the contact diameter. The track had worn unevenly along its length (as well as its width): the right side still appeared to have coating remaining, while the left side had gold-colored (dark) areas where the TiN layer was visible, as well as a bright, shiny spot. Raman spectra from the track were similar to the as-deposited MoS_2, even in the areas where TiN was observed optically. SAM of the latter region revealed that while MoS_2 was still on the track surface, both TiN and steel Fe(Cr) oxide were exposed in some of the thinned areas. EDS estimates of the average thickness of MoS_2 remaining at various points along the wear track are plotted in Fig. 7.

On the ball surface, debris had accumulated in and around the contact zone. Raman spectra indicated that the debris in the contact zone consisted of MoS_2 and some graphite-like material; EDS revealed Mo and S with some C and O present, and SAM spectra also suggested mixed MoS_2 and graphite-like carbon. Thickness of the debris on the ball was estimated from the integrated EDS Mo+S peak intensity. The average thickness in the center of the wear scar was ~7 nm, while small patches of debris and the material around the edges were found to be considerably thicker. None of the analytical techniques detected the presence of Ti (from the TiN layer) on the ball, indicating that only MoS_2 was worn from the track. A summary of compositions identified on the track and ball surfaces is presented in Table 1.

The μ and R_c behavior can be accounted for by the compositions and thicknesses of the worn surfaces. Since both μ and R_c data were reproducible over the last 20-30 sliding cycles,

variations in μ and R_c during the last sliding cycle can be associated with wear track features rather than the ball transfer film evolution. The friction coefficient was higher on the left side of the wear track, where the MoS_2 coating had thinned considerably, exposing TiN and steel. Thus, higher local friction coefficient was due to MoS_2 on the ball rubbing part of the time on exposed TiN and/or steel on the track. On the other hand, the R_c data showed the lowest values on the left (thinned) side of the track, and highest values on the thicker side. Furthermore, the shape of the EDS MoS_2 thickness vs. position data was remarkably similar to the shape of R_c vs. position on the wear track (see Figs. 5b and 7); this suggests that changes in R_c might be due to variations in wear track thickness.

The resistivity of the interfacial film separating the steel ball and substrate can be estimated by correlating R_c and thickness data. The resistance through a contact is controlled by the contact area, *A*, the thickness of the interfacial film, *t*, and the resistivity of the film, ρ. In the simplest case, this relationship can be represented as

$$R_c = \frac{\rho \cdot t}{A}. \qquad (1)$$

For MoS_2, the Hertzian area is a reasonable estimate of the contact area [25]. The interfacial film thickness was estimated as $t_{transfer} + t_{coating}$, where $t_{transfer}$ ~7 nm and $t_{coating}$ values are given in Fig. 7. This combined thickness, together with the R_c values as a function of position along the track (Fig. 5b), were used to calculate ρ by Eq. 1. We obtained an average value of ~75 Ωm for the resistivity of the interface material. For reference, the resistivity of single crystal MoS_2 is very anisotropic: 63 Ωm (perpendicular) and 0.015 (parallel) to the basal planes [26]. The other interface material, TiN, should have resistivity several orders lower (~10^{-7} Ωm [27]). The resistivity of the interfacial film agrees remarkably well with that of basal-oriented MoS_2. While we haven't measured the perpendicular resistivity of our coatings, we know that prior to sliding the IBAD MoS_2 coating is basally oriented and fully dense [28], and that during sliding MoS_2 transfer films orient with the basal planes parallel to the sliding interface [29,30]. This result, while singular, is encouraging and suggests that R_c might be used to quantitatively monitor coating wear.

3.2.2. Analysis and interpretation of 2048 cycle track

The last pass μ and R_c data are shown in Fig. 8. The friction coefficient was high and uneven across the track, with largest values near the turnaround points. Contact resistance was fairly uniform across the track, except at the left end of the track at the onset of sliding.

Optical micrographs of the ball and track surfaces are shown in Fig. 9. In the micrograph, the wear track appears bright and shiny, except where covered by dark (reddish-brown) patches. Some of the TiN layer was visible (gold) at the extreme edges of the track. Both Raman and SAM confirmed that the shiny areas of the track were depleted of MoS_2 and TiN, with iron oxide as the predominant species on both the shiny areas and dark patches. The ball surface was rough and heavily worn, with copious debris surrounding the contact zone. Raman and SAM analyses indicated only iron oxide debris in the contact zone, although some MoS_2 remained in debris outside the contact zone. Raman spectra also showed the presence of graphite-like material in the debris. EDS indicated that the center of the ball wear scar contained some Ti (from the TiN layer), hence TiN as well as MoS_2 were worn from the track. A summary of surface compositions identified on the track and ball surfaces is presented in Table 2.

No correlation between the last pass friction and R_c is obvious. However, higher friction was found at regions of the track with higher concentrations of brown patches (oxides); this behavior is consistent with earlier studies showing that friction coefficients for steel vs. steel can vary between 0.2 and 0.6 depending on the phase of the third body oxide debris [31,32]. In addition, the resistance of the contact can be influenced by oxides in the interface. Therefore, the buildup of oxide debris can account for both the friction coefficient as well as the relatively high R_c late in sliding.

3.3. Interpretation of triboscopy images

3.3.1. 512 Cycle Test

The higher friction on the left side of the track as early as 100 cycles suggests that the coating began to thin there, leading to bare TiN patches by 512 cycles; this is also consistent with lower R_c values on that side during the test. The regions of very low R_c (Fig. 2, B) occurred intermittently at locations along the track where exposed TiN and steel were observed. We speculate that these regions indicate breakthrough of the MoS_2 coating to the TiN layer, while

recovery (low to higher R_c) is associated with replenishment of MoS_2 to either the track or the ball. Since our observations showed that the track had exposed TiN and steel even *after* R_c had recovered, healing of the worn track surfaces by retransfer of MoS_2 was not likely responsible for recovery. Instead, recovery was probably due to reapplication or redistribution of MoS_2 on the *ball*. Redistribution of lubricant on the ball is consistent with the observations of both Sliney [33] and Berthier [34], who by optical observations through transparent concentrated contacts demonstrated the ease of plastic deformation and flow of MoS_2.

While the above interpretation of the reductions in R_c could be attributed to localized coating wear observed on the worn track surface, we cannot account for the very high resistivity observed early in sliding (Fig. 2, A). No gradient in friction was observed in the corresponding friction image and, when the test was stopped, the worn surface in this area was nearly as thick as when sliding began. An extremely thick transfer film, constriction resistance, or even a bit of oxide debris or dust trapped on the track might account for this feature.

3.3.2. 2048 Cycle Test

Early on, sliding took place between MoS_2 on the track and on the ball, and the friction and R_c data exhibited similar behavior to the 512 cycle test. As more MoS_2 was worn away and the underlying TiN and steel were exposed, the μ and R_c images became noisier. By the end of the test, only oxidized steel and iron oxide debris remained; then, sliding was controlled by these oxide surface films and μ and R_c were erratic. We speculate that the variation in μ and R_c at the end of the test was related to the buildup and loss of these oxide films within the sliding interface.

3.3. Implications

These experiments have demonstrated that the electrical contact resistance of steel vs. MoS_2 contacts was sensitive to changes occurring early in sliding, generally well before the friction signal was affected. This was true for both averaged data and triboscopy images; the latter, however, added a means of monitoring specific locations along the tracks where μ and R_c variations were taking place. Regions of low relative R_c values (either localized as shown in Fig. 2, region B and Fig. 4, or as a gradient along the track, Fig. 5b) were attributed to thinning of the MoS_2 coating. Friction was not significantly affected in these thinned regions; recent studies of lubrication by MoS_2 films have revealed that as few as 1 or 2 monolayers can provide low friction

sliding [11]. Thus R_c may provide a more sensitive means of monitoring wear or degradation of MoS_2 coatings, where redistribution of lubricant through transfer processes may mask the location of damaged regions for thousands of cycles [6]. In addition, the sensitivity of R_c to contact changes suggests that R_c measurements would be suitable for tracking performance of remotely deployed bearings (e.g. satellite gimbals), where monitoring coating damage and predicting the remaining useful lifetime would be advantageous. Based on the present experimental results, further investigation of triboscopy for failure prediction of solid lubricants seems warranted.

4. Summary and Conclusions

Data from real time, spatially resolved friction and electrical contact resistance measurements were coupled with *ex situ* optical and chemical analyses of worn surfaces. The friction coefficient of steel vs. MoS_2 in ambient air was insensitive to substantial changes in MoS_2 thickness and even to localized damage in the MoS_2 coating. In contrast, contact resistance was sensitive to changes in the contact early in sliding life, suggesting that monitoring the contact resistance may provide a better means of predicting failure in MoS_2 sliding contacts than friction alone.

From these experiments, a number of conclusions can be drawn:

1. Both averaged and spatially resolved electrical contact resistance measurements were more sensitive to MoS_2 coating loss or damage than friction force measurements.
    - local fluctuations (both low and high) of R_c were observed long before any rises or fluctuations in μ
    - local drops in R_c were detected as early as 300 sliding cycles.
2. Friction coefficient was insensitive to changes in MoS_2 coating thickness until a significant area of underlying materials were exposed.
3. Recovery of both localized high μ and low R_c regions occurred.
4. R_c was correlated to wear track thickness and may furnish an indication of early coating wear that μ cannot provide.

Acknowledgments

The authors acknowledge ONR (K.J.W. and I.L.S.) and CNRS (M.B.) for funding. We also thank R.N. Bolster and L.E. Seitzman for valuable assistance in coating deposition and characterization, and D.N. Dunn for critical comments on the manuscript.

References

[1] T. Spalvins, Frictional and morphological properties of Au-MoS_2 films sputtered from a compact target, *Thin Solid Films, 118* (1984) 375-384.
[2] G.D. Gamulya, G.V. Dobrovol'skaya, I.L. Lebedeve and T.P. Yukhno, General characteristics of wear in vacuum for solid film lubricants formulated with lamellar materials, *Wear, 93* (1984) 319-332.
[3] P.D. Fleischauer and R. Bauer, Chemical and structural effects on the lubrication properties of sputtered MoS_2 films, *Tribol. Trans., 31* (1988) 239-250.
[4] M.R. Hilton, R. Bauer, and P.D. Fleischauer, Tribological performance and deformation of sputter-deposited MoS_2 solid lubricating films during sliding wear and indentation contact, *Thin Solid Films, 188* (1990) 219-236.
[5] G.B. Hopple, J.E. Keem, and S.H. Lowenthal, Development of fracture resistant, multilayer films for precision ball bearings, *Wear, 162-164* (1993) 919-924.
[6] K.J. Wahl and I.L. Singer, Quantification of a lubricant transfer process that enhances the sliding life of a MoS_2 coating, *Tribology Letters, 1* (1995) 59-66.
[7] E.W. Roberts and M.J. Todd, Space and vacuum tribology, *Wear, 136* (1990) 157-167.
[8] M.R. Hilton and P.D. Fleischauer, Lubricants for high-vacuum applications, Aerospace Technical Report TR-0091 (6945-03)-6 (1993).
[9] P.D. Ehni and I.L. Singer, Composition of sputter deposited MoS_2 films during run-in in vacuum, in L.E. Pope, L. Fehrenbacher, and W.O. Winer, (eds.), *New Materials Approaches to Tribology: Theory and Applications*, Materials Research Society Symposium Proceedings, MRS, Pittsburgh, Vol. 140, 1989, pp. 245-250.
[10] R.L. Fusaro, Lubrication and failure mechanisms of molybdenum disulfide films. II - Effect of substrate roughness, *ASLE Trans., 25* (1982) 141-156.
[11] I.L. Singer, T. Le Mogne, C. Donnet, and J.M Martin, In situ analysis of the tribochemical films formed by SIC sliding against Mo in partial pressures of SO_2, O_2, and H_2S gases, *J. Vac. Soc. Technol. A, 14* (1996) 38-45.
[12] F.P. Bowden and D. Tabor, *The Friction and Lubrication of Solids*, Part I, Clarendon Press, Oxford, 1986, pp.108-109.
[13] R. Holm, *Electric Contacts, Theory and Application*, Springer Verlag, New York, 1967.
[14] M.J. Furey, Metallic contact and friction between sliding surfaces, *ASLE Transactions, 4* (1961) 1-11.
[15] Y. Wantanabe, Sliding contact characteristics between composite materials containing layered solid lubricants and carbon, *Wear, 155* (1992) 237-249.
[16] C. Gao, L. Bredell, D. Kuhlmann-Wilsdorf and D. Makel, Micromechanics of MoS_2 lubrication, *Wear, 162-164* (1993) 480-491.
[17] M. Belin and J.M. Martin, Triboscopy, a new approach to surface degradations of thin films, *Wear, 156* (1992) 151-160.
[18] R.N. Bolster, I.L. Singer, J.C. Wegand, S. Fayeulle, and C.R. Gossett, Preparation by ion-beam-assisted deposition, analysis and tribological behavior of MoS_2 films, *Surf. Coat. Technol., 46* (1991) 207-216.
[19] L.E. Seitzman, R.N. Bolster, and I.L. Singer, Effects of temperature and ion-to-atom ratio on the orientation of IBAD MoS_2 coatings, *Thin Solid Films, 260* (1995) 143-147.
[20] L.E. Seitzman, I.L. Singer, R.N. Bolster, and C.R. Gossett, Effect of a titanium nitride interlayer on the endurance and composition of a molubdenum disulfide coating prepared by ion-beam-assisted deposition, *Surf. Coat. Technol., 51* (1992) 232-236.
[21] C. Pritchard and J.W. Midgely, The effect of humidity on the friction and life of unbonded molybdenum disulphide films, *Wear, 156* (1969) 39-50.
[22] V. Hopkins and M. Campbell, Film thickness effect on the wear life of a bonded solid lubricant film, *Lubr. Eng., 25* (1969) 15-24.
[23] P.D. Ehni and I.L. Singer, Electron-beam microprobe analysis of the wear behavior of sputter-deposited MoS_2 coatings, *Appl. Surf. Sci., 59* (1992) 45-53.
[24] K.J. Wahl and I.L. Singer, Role of the third body in life enhancement of MoS_2, in D. Dowson, (ed.), "The Third Body Concept: Interpretation of Tribological Phenomena," Vol. 31, New York, Elsevier, 1996, pp. 407-413.
[25] I.L. Singer, R.N. Bolster, J. Wegand, S. Fayeulle, and B.C. Stupp, Hertzian stress contribution to low friction behavior of thin MoS_2 coatings, *Appl. Phys. Lett., 57* (1990) 995-997.

[26] B. Bhushan and B.K. Gupta, *Handbook of Tribology*, McGraw-Hill, New York 1991, p. 5.17.
[27] *CRC Handbook of Chemistry and Physics, 75th edition*, ed. D.R. Lide, CRC Press, Boca Raton, 1994.
[28] L.E. Seitzman, R.N. Bolster, I.L. Singer, and J.C. Wegand, Relationship of endurance to microstructure of IBAD MoS_2 coatings, *Tribology Trans., 38* (1995) 445-451.
[29] D. Godfrey and E.E. Bisson, Bonding of molybdenum disulphide to various materials to form a solid lubricating film, NACA TN 2628, 1952.
[30] M.R. Hilton and P.D. Fleischauer, Structural studies of sputter-deposited MoS_2 solid lubricant films, in L.E. Pope, L. Fehrenbacher, and W.O. Winer, (eds.), *New Materials Approaches to Tribology: Theory and Applications*, Materials Research Society Symposium Proceedings, MRS, Pittsburgh, Vol. 140, 1989, pp. 227-238.
[31] S. Fayeulle and I.L. Singer, Friction behavior and debris formation of titanium-implanted 52100 steel, *Materials Sci. and Engineering A115* (1989) 285-290.
[32] I.L. Singer and R.A. Jeffries, Composition and sliding contact behavior of oxidized titanium-implanted 52100 steel, *Materials Sci. and Engineering A115* (1989) 279-284.
[33] H.E. Sliney, Dynamics of solid lubrication as observed by optical microscopy, *ASLE Trans., 21* (1977) 109-117.
[34] A. Jullien, M.H. Meurisse, Y. Berthier, Determination of tribological history and wear through visualisation in lubricated contacts using a carbon-based composite, *Wear, 194* (1996) 116-125.

Tables

Table 1. Compositions of 512 cycle ball and track surfaces inferred from surface analyses.

Technique	Ball	Track
micro-Raman	MoS_2 C (graphite-like)	MoS_2
EDS	Mo+S, some C,O	Mo+S, Ti
SAM	MoS_2	MoS_2 Fe(Cr) oxide and TiN

Table 2. Compositions of 2048 cycle ball and track surfaces inferred from surface analyses.

Technique	Ball	Track
micro-Raman	C (graphite-like) + Fe_2O_3 MoS_2 (only at sides)	Fe_2O_3 no MoS_2
EDS	center highly oxidized small Mo+S, Ti	--
SAM	Fe oxide	Fe(Cr) oxide no MoS_2 or TiN

Figure Captions

Figure 1. (a) Average friction coefficient, μ^{av} and (b) electrical contact resistance, R_c^{av} for steel balls sliding against 55 nm thick MoS_2 in 60% RH air. The examples shown were run to 512 and 2048 cycles.

Figure 2. Triboscopic images for μ and R_c for the 512 cycle test from Fig. 1. Gray-scale calibration bars for μ and R_c are shown beneath the images.

Figure 3. Composite triboscopic images for μ and R_c for the 2048 cycle test from Fig. 1. Gray-scale calibration bars for μ and R_c are shown beneath the images.

Figure 4. Composite triboscopic R_c image from a test run to 1536 cycles at 10 N load. The calibration bar for R_c is shown beneath the image.

Figure 5. Spatially resolved (a) μ and (b) R_c, as a function of track position, for the last sliding pass before the 512 cycle test was stopped.

Figure 6. Optical micrographs of (a) ball and (b) track surfaces for the steel ball against MoS_2 after 512 sliding cycles.

Figure 7. Average thickness of MoS_2 coating in wear track, as determined by integration of the EDS (Mo+S) intensity [see text for details].

Figure 8. Spatially resolved (a) μ and (b) R_c, as a function of approximate track position, for the last sliding pass before the 2048 cycle test was stopped.

Figure 9. Optical micrographs of (a) ball and (b) track surfaces for the steel ball against MoS_2 after 2048 sliding cycles.

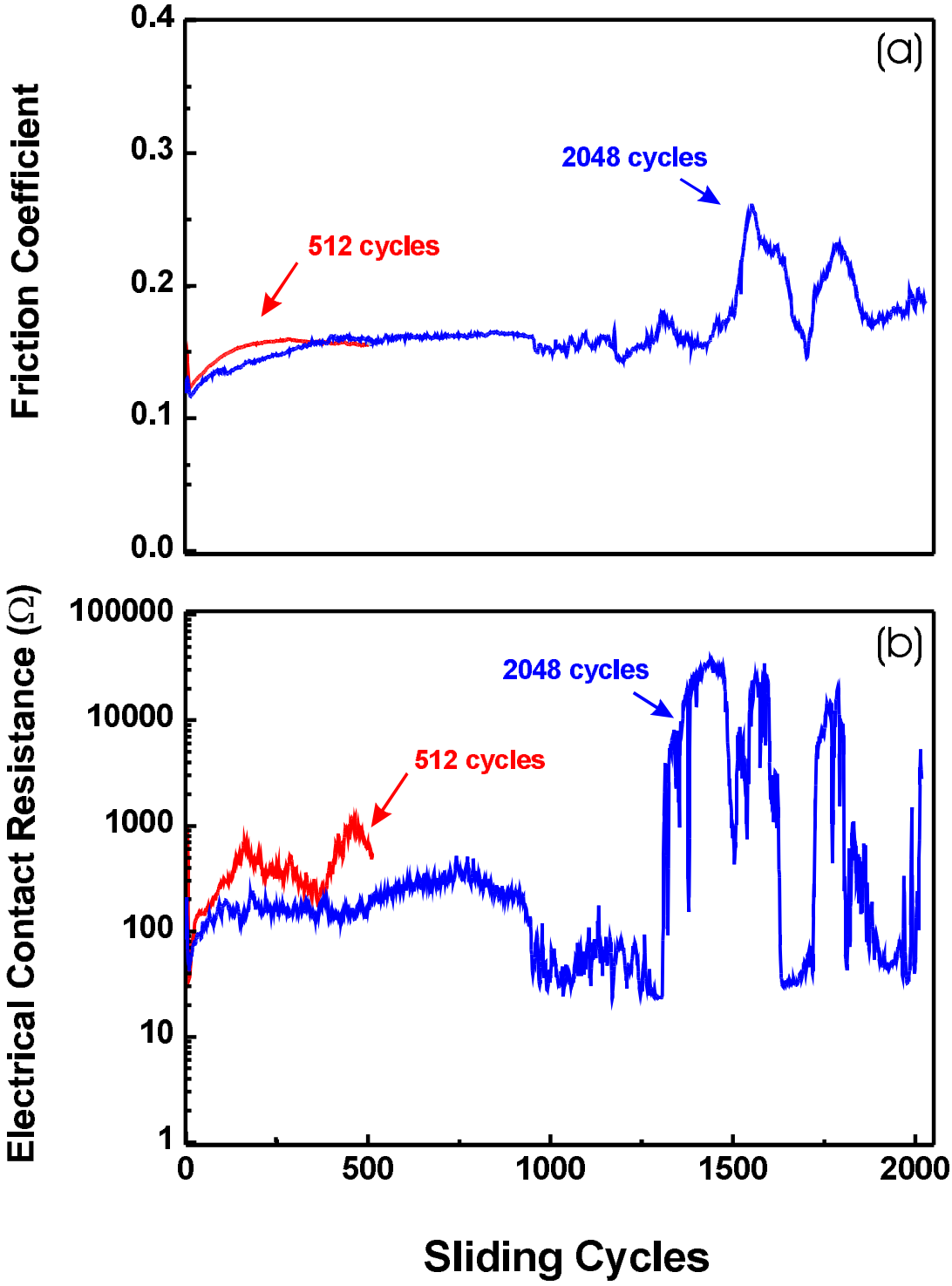

Figure 1. (a) Average friction coefficient, μ^{av} and (b) electrical contact resistance, R_c^{av} for steel balls sliding against 55 nm thick MoS_2 in 60% RH air. The examples shown were run to 512 and 2048 cycles.

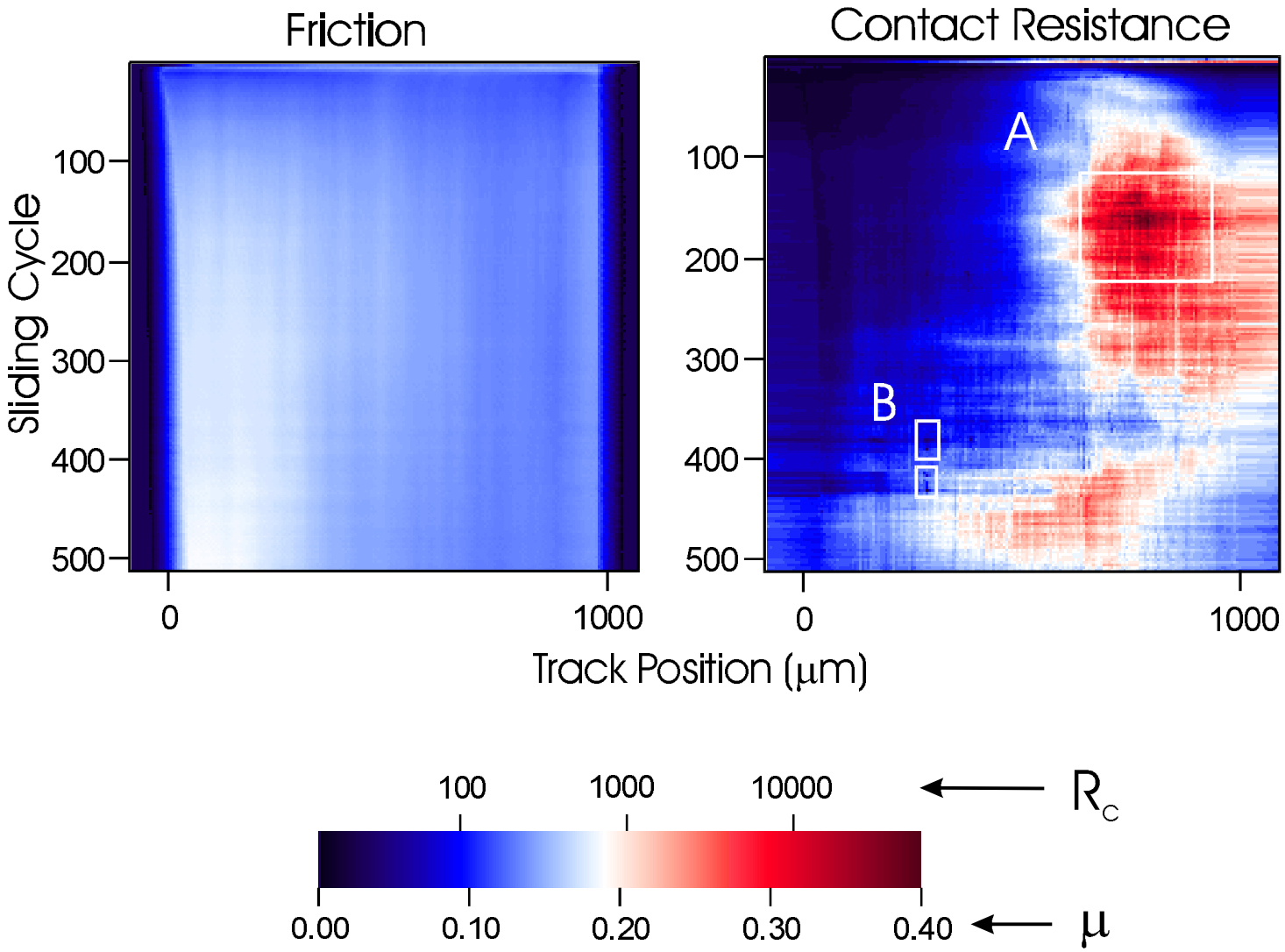

Figure 2. Triboscopic images for μ and R_c for the 512 cycle test from Figure 1. Gray-scale calibration bars for μ and R_c are shown beneath the images.

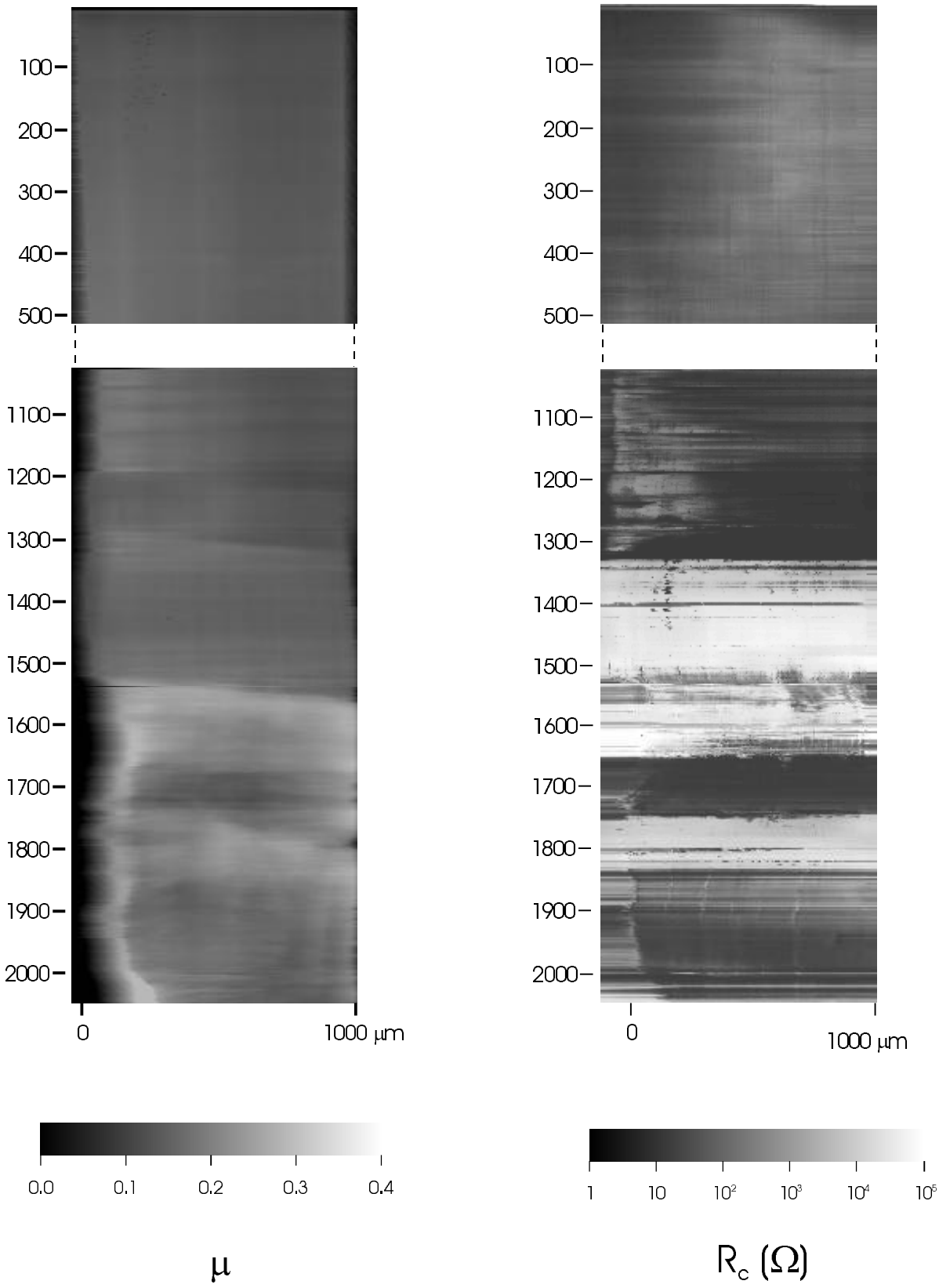

Figure 3. Composite triboscopic images for μ and R_c for the 2048 cycle test from Figure 1. Gray-scale calibration bars for μ and R_c are shown beneath the images.

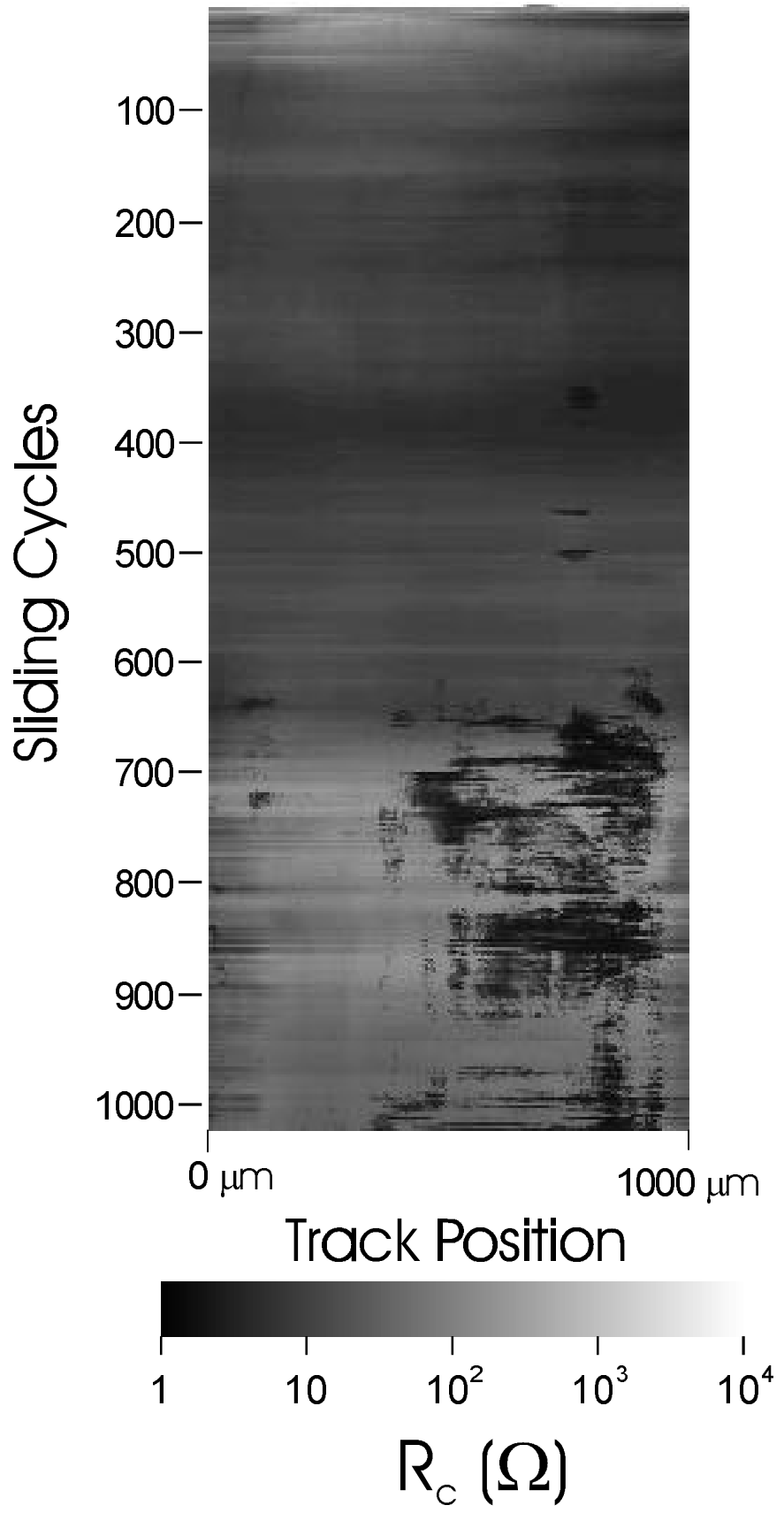

Figure 4. Composite triboscopic R_c image for a test run to 1536 cycles at 10N load. Gray-scale calibration bars for μ and R_c are shown beneath the image.

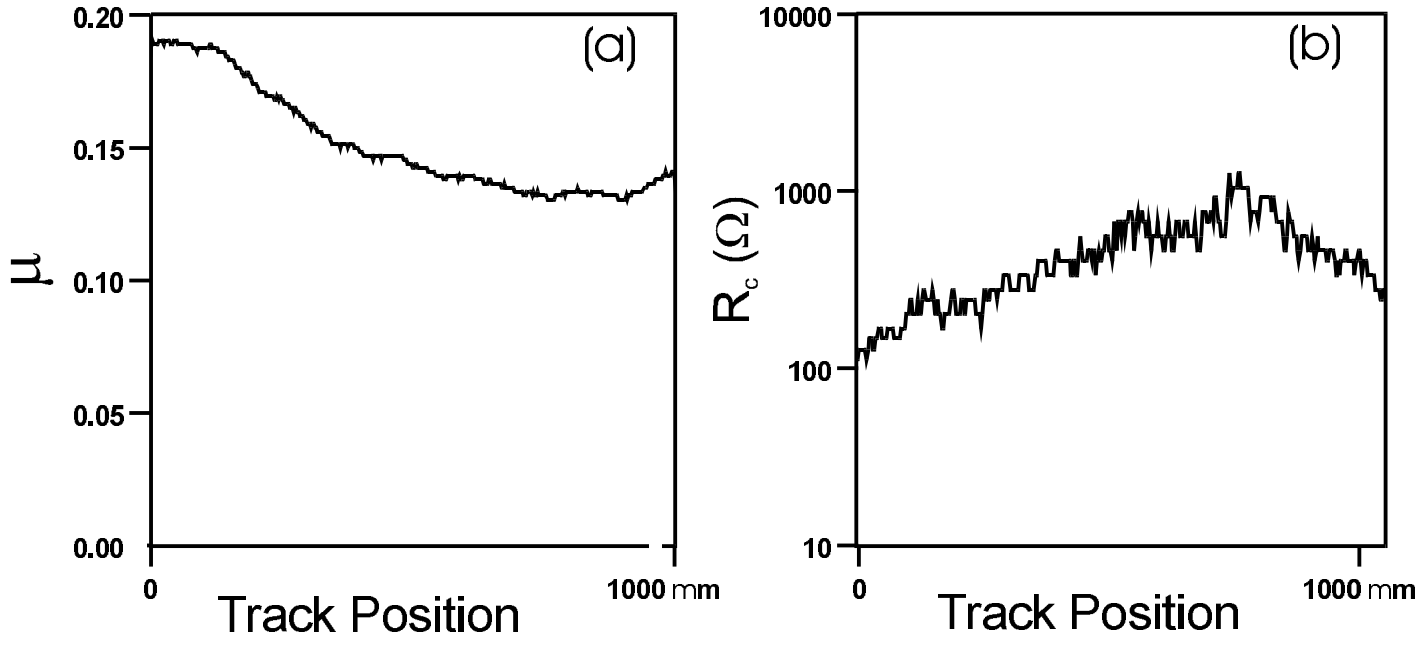

Figure 5. Spatially resolved (a) μ and (b) R_c, as a function of track position, for the last sliding cycle before the 512 cycle test was stopped.

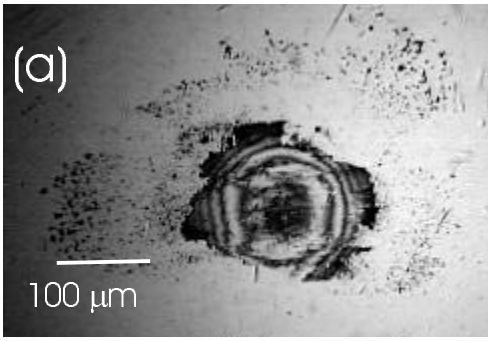

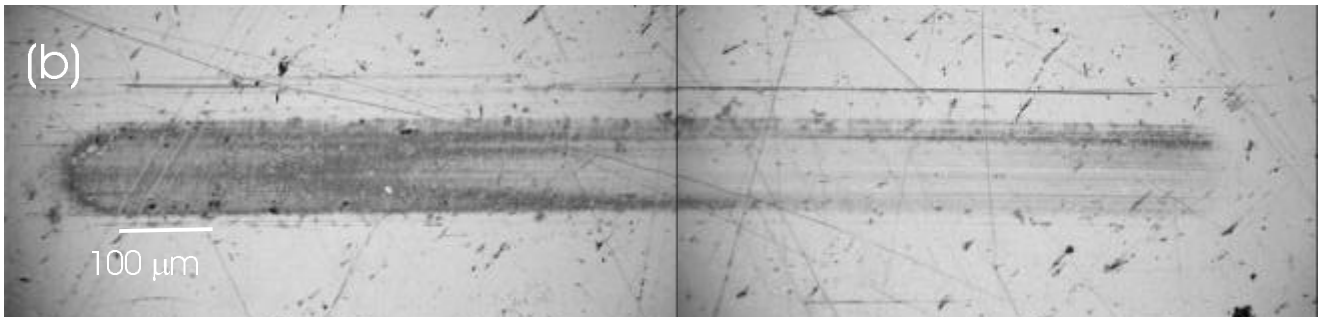

Figure 6. Optical micrographs of (a) ball and (b) track surfaces for the steel ball against MoS_2 after 512 sliding cycles.

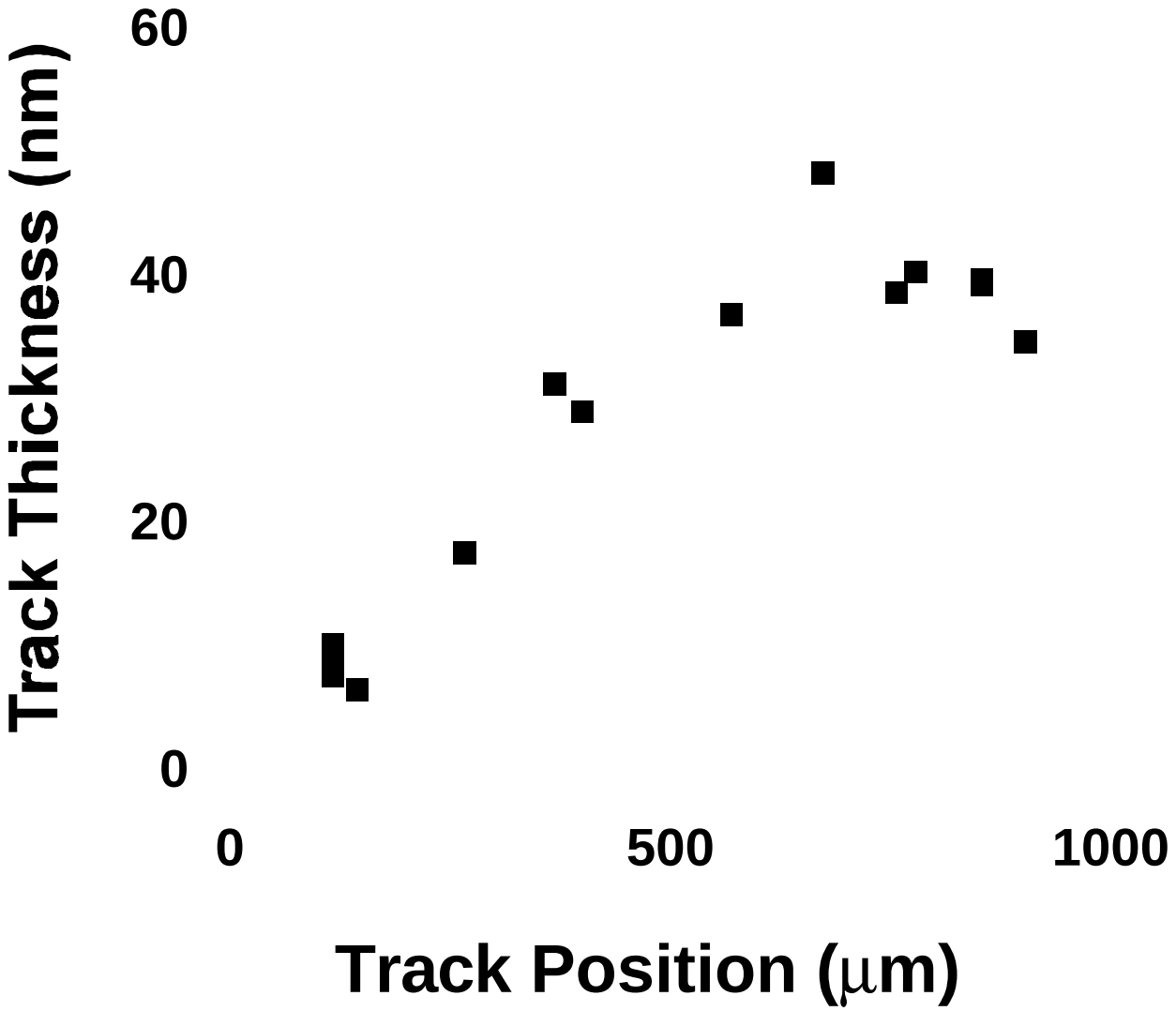

Figure 7. Average thickness of MoS_2 coating in wear track, as determined by integration of the EDS (Mo + S) intensity.

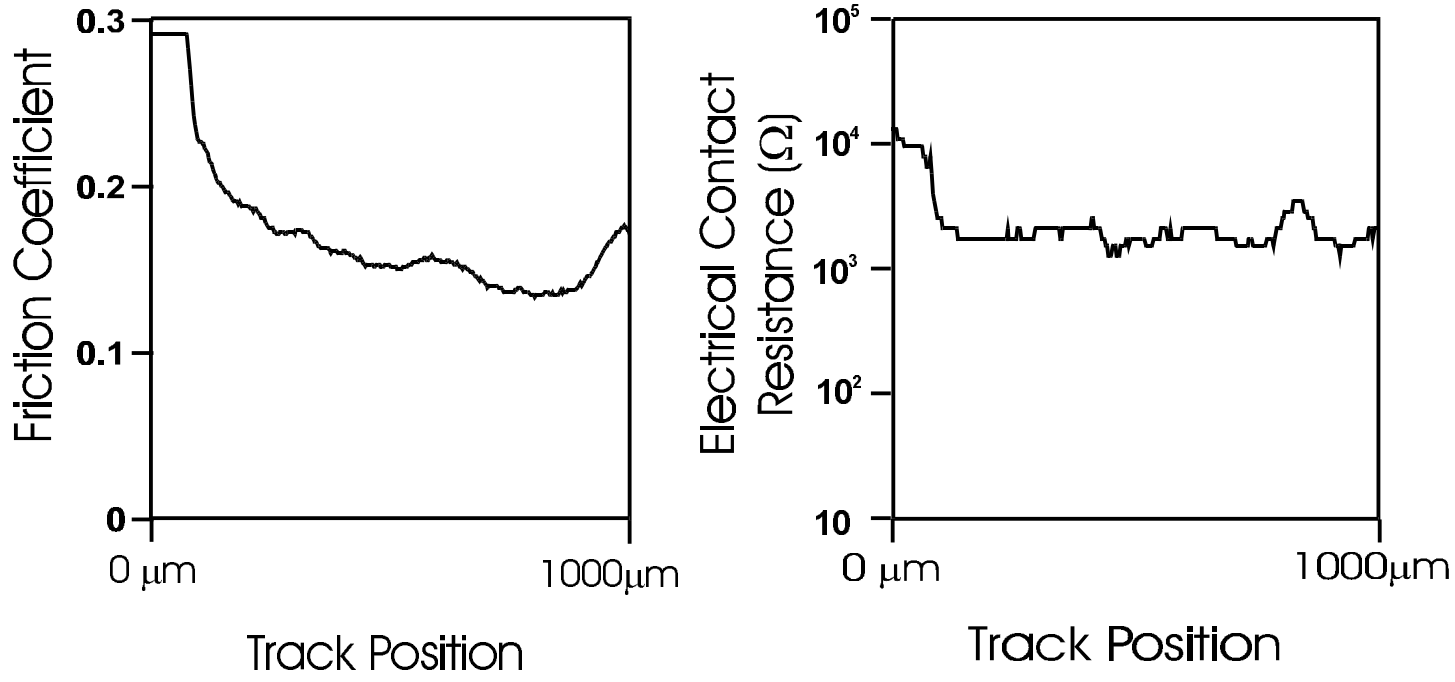

Figure 8. Spatially resolved (a) μ and (b) R_c, as a function of approximate track position, for the last sliding pass before the 2048 cycle test was stopped.

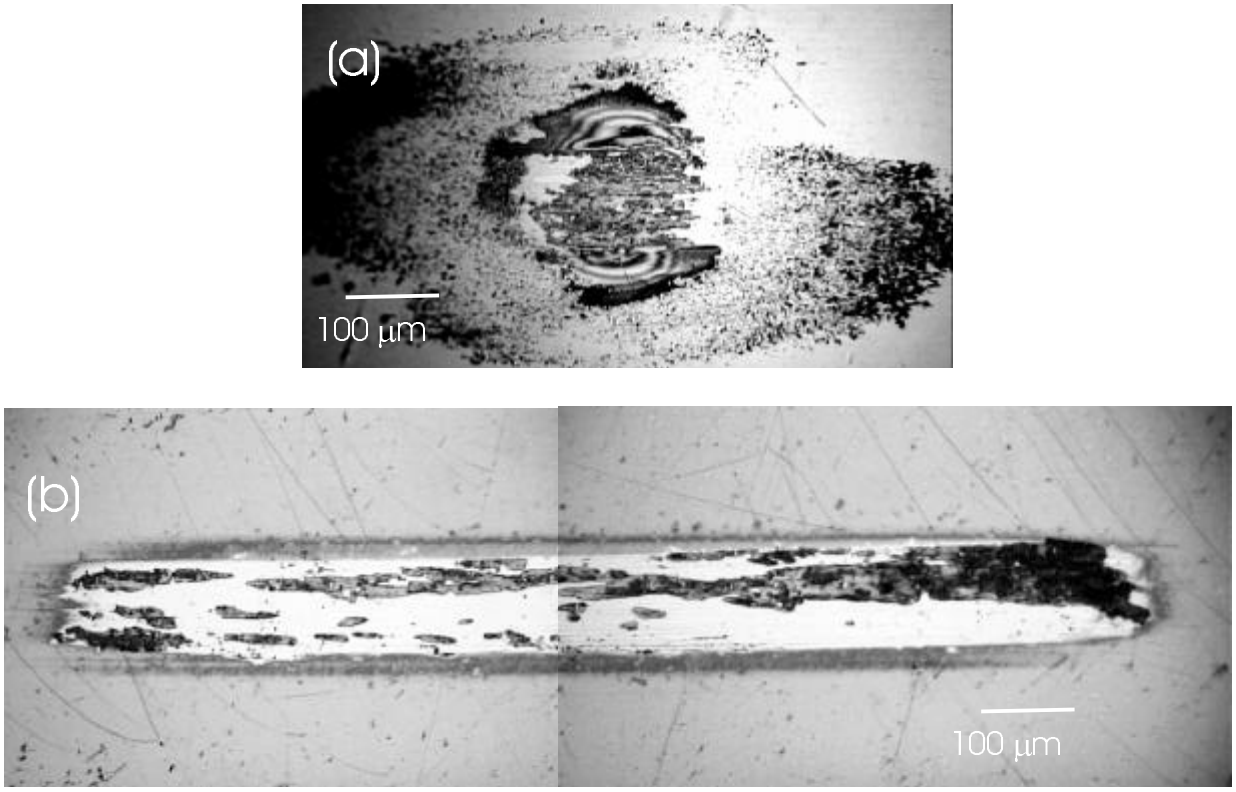

Figure 9. Optical micrographs of (a) ball and (b) track surfaces for the steel ball against MoS_2 after 2048 sliding cycles.